Gergely KOVÁCS, Miklós KUCZMANN

Széchenyi István University

Solution of the TEAM workshop problem No. 7 by the Finite Element Method

Abstract. *This paper presents some potential formulations which can be derived from the „quasi-static" Maxwell's equations. The simulation results of the potential formulations are compared with each others focusing their CPU times and their accuracy – and with the measurement results, as well. The model –which was simulated - the TEAM workshop problem No. 7. The magnetic flux density and the eddy current were shown by the results of the simulation.*

Streszczenie. *W artykule przedstawiono sformułowania potencjałowe wyprowadzone z quasi-statycznych równań Maxwella. Wyniki symulacji sformułowań potencjałowych są porównywane między sobą w aspekcie czasu CPU i dokładności oraz z wynikami pomiarów. Model symulowany w tej pracy pochodzi z katalogu problemów sformułowanych przez TEAM Workshop i ma numer 7. Pokazano strumień magnetyczny oraz prądy wirowe.(**Rozwiązanie problem Nr 7 TEAM Workshop metodą elementów skończonych**)*

Keywords: TEAM workshop problem 7, eddy current field, potential formulations, finite element method.
Słowa kluczowe: problem 7 TEAM, pole prądów wirowych, sformułowania potencjałowe, metoda elementów skończonych

Introduction

The idea of the TEAM (testing electromagnetic analysis methods) exercises is issues to the Argonne National Laboratory. The aim of these initiations was to disperse and to propagate the usage of the numerical techniques. By resolving more types exercises the accuracy of the results can be confirmed. The benchmark problem No. 7 of the TEAM workshop consists of an aluminium plate with a hole and a coil [1-5]. The sketched model can be seen in Fig. 2.

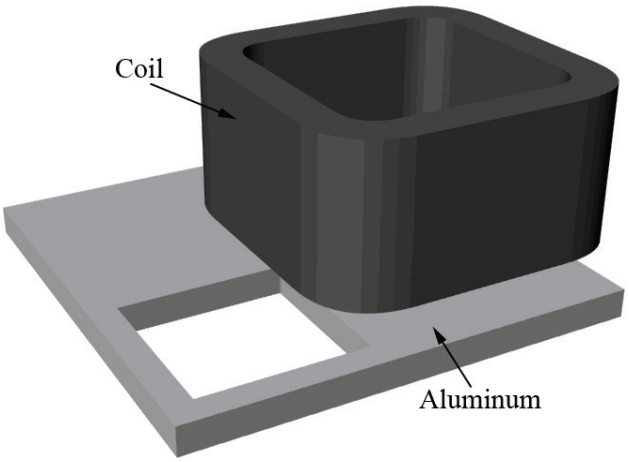

Fig.1. The drawn model

The coil is excited by a sinusoidal current which generates a time varying magnetic field in the vicinity of the coil. This field induces eddy currents inside a conducting material, which currents generate a magnetic field, and this field modifies the magnetic field supplied by the sources. The conductivity of the plate is 3,526x10^7 S/M. The source of the magnetic field is a sinusoidal current. The maximum ampere turn is 2742; the frequencies are 50Hz and 200Hz.

The benchmark problem No.7 has measurement results as well. One of the aims was simulating the measurement results, helped by the finite element methods, what can be derived from the potential formulations. The results were calculated by the help of some different potential formulations ($\vec{A},V$ - $\vec{A}$, $\vec{T},\Phi-\Phi$) [6-7]. The other aim was comparing these potential formulations with each other, and considering their CPU times and their accuracy with the measurements results. In this paper the comparisons and the potential formulations are also presented.

Potential formulations

The eddy current field or the quasi-static magnetic field can be derived from the potential formulations more ways [7]. It can be derived from the magnetic vector potential $\vec{A}$ which is expanded with the electric scalar potential V, respectively, it can be employed the current vector potential $\vec{T}$ expanded with the reduced magnetic scalar potential Φ. In case of the quasi-static magnetic field the domains of the model can be divided (see in Fig.2.).

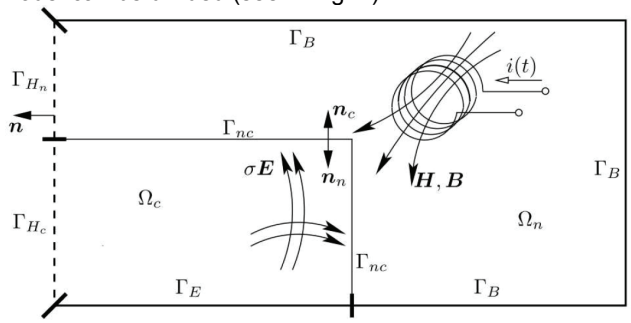

Fig.2. Structure of an eddy current field problem

Here Ω_c means the conducting domain and Ω_n means the non-conducting domain. The boundary of the eddy current free domain was signed by Γ_B, where the normal component of the magnetic flux is zero. The boundary of the eddy current domain was signed by Γ_E. In the case of this boundary the tangential component of the electric field is zero. The symmetry planes were signed by Γ_{Hc} and Γ_{Hn}, where the tangential component of the magnetic field is zero. The potential formulations can be approximate with nodal elements or edge elements [7-8].

From the Maxwell's equations the gauged $\vec{A},V$ - $\vec{A}$ potential formulation can be derived [7-8]. The applied Maxwell's equations are

$$\nabla\times\vec{H}=\vec{J}\ \text{in}\ \Omega_c, \tag{1}$$

(2) $$\nabla \times \vec{H} = \vec{0} \text{ in } \Omega_{\mathrm{n}},$$

(3) $$\nabla \times \vec{E} = -\mathrm{j}\omega \vec{B} \text{ in } \Omega_{\mathrm{c}},$$

(4) $$\nabla \cdot \vec{B} = 0 \text{ in } \Omega,$$

(5) $$\nabla \cdot \vec{J} = 0 \text{ in } \Omega.$$

These linear static and "quasi-static" Maxwell's equations can be used to simulate linear eddy current field problems. Here $\vec{H}$ is the magnetic field intensity, $\vec{J}_0$ is the source current density, $\vec{J}$ is the eddy current density, $\vec{E}$ is the electric field intensity, and finally $\vec{B}$ is the magnetic flux density. The magnetic vector potential can be described in the Ω_{n} non-conducting domain and in the Ω_{c} conducting domain as well, and the electric scalar potential can be described only the Ω_{c} conducting domain. The magnetic field intensity can be described by

(6) $$\vec{H} = \nu \vec{B},$$

where ν is the reluctivity. The eddy current density can be obtained,

(7) $$\vec{J} = \sigma \vec{E},$$

where σ is the conductivity. The magnetic flux density can be expressed as

(8) $$\vec{B} = \nabla \times \vec{A},$$

which satisfies (4), because of the identity $\nabla \cdot \nabla \times \vec{v} \equiv 0$ for any vector function $\vec{v} = \vec{v}\left(\vec{r}\right)$. Substituting (8) to the (1) and (2) and using the (6), constitutive relation can be obtained by the following partial differential equations, where $\nabla \cdot \vec{A} = 0$ Coulomb gauge is satisfied:

(9) $$\nabla \times \left(\nu \nabla \times \vec{A}\right) + \sigma\left(\mathrm{j}\omega \vec{A} + \nabla V\right) - \nabla\left(\nu \nabla \cdot \vec{A}\right) = 0 \text{ in } \Omega_{\mathrm{c}},$$

and

(10) $$\nabla \times \left(\nu \nabla \times \vec{A}\right) - \nabla\left(\nu \nabla \cdot \vec{A}\right) = \vec{J}_0 \text{ in } \Omega_{\mathrm{n}}.$$

Using the (3) and (8) equations for the electric scalar potential can be expressed as

(11) $$\vec{E} = -\mathrm{j}\omega \vec{A} - \nabla V.$$

Substituting (11) to (7) and using (5) the following partial differential equation can be obtained:

(12) $$-\nabla \cdot (\sigma \mathrm{j}\omega \vec{A} + \sigma \nabla V) = 0, \text{ in } \Omega_{\mathrm{c}}.$$

The weak formulations from the partial differential equations (9), (10), and (12), in the case of the gauged $\vec{A},V$ - $\vec{A}$ potential formulation, are these follows:

$$\int_{\Omega_{\mathrm{c}} \cup \Omega_{\mathrm{n}}} \left[\nu(\nabla \times \vec{W}) \cdot (\nabla \times \vec{A})\right] + \nu \nabla \cdot \vec{W}\, \nabla \cdot \vec{A}\, \mathrm{d}\Omega$$

(13) $$+ \int_{\Omega_{\mathrm{c}}} \vec{W} \cdot \left(\sigma \mathrm{j}\omega \vec{A} + \sigma \nabla V\right) \mathrm{d}\Omega = \int_{\Omega_{\mathrm{n}}} \vec{W} \cdot \vec{J}_0 \mathrm{d}\Omega,$$

and

(14) $$\int_{\Omega_{\mathrm{c}}} \nabla \mathrm{N} \cdot \left(\sigma \mathrm{j}\omega\, \vec{A} + \sigma \nabla V\right) \mathrm{d}\Omega = 0.$$

From the Maxwell's equations, the ungauged $\vec{A},V$ - $\vec{A}$ potential formulation can be derived in the similar way. However in this case the source current density can be represented by [8]

(15) $$\vec{J}_0 = \nabla \times \vec{T}_0,$$

where the current vector potential is

(16) $$\nabla \times \vec{T} = 0 \text{ in } \Omega_{\mathrm{c}},$$

or

(17) $$\nabla \times \vec{T} = \vec{J}_0 \text{ in } \Omega_{\mathrm{n}}.$$

In the case of ungauged $\vec{A},V$ - $\vec{A}$ potential formulation the Coulomb-gauge is satisfied automatically, consequently the equations (9) and (10) are changed:

(18) $$\nabla \times \left(\nu \nabla \times \vec{A}\right) + \sigma\left(\mathrm{j}\omega \vec{A} + \nabla V\right) = 0 \text{ in } \Omega_{\mathrm{c}},$$

and

(19) $$\nabla \times \left(\nu \nabla \times \vec{A}\right) = \nabla \times \vec{T}_0 \text{ in } \Omega_{\mathrm{n}}.$$

The weak formulations the (18) and (19) partial differential equations in the case of the ungauged $\vec{A},V$ - $\vec{A}$ potential formulation are the follows:

$$\int_{\Omega_{\mathrm{c}} \cup \Omega_{\mathrm{n}}} \left[\nu(\nabla \times \vec{W}) \cdot (\nabla \times \vec{A})\right] \mathrm{d}\Omega$$

(20) $$+ \int_{\Omega_{\mathrm{c}}} \vec{W} \cdot \left(\sigma \mathrm{j}\omega \vec{A} + \sigma \nabla V\right) \mathrm{d}\Omega = \int_{\Omega_{\mathrm{n}}} \vec{T}_0 \cdot \left(\nabla \times \vec{W}\right) \mathrm{d}\Omega.$$

The other weak form is equal to the (14) equation.

From the Maxwell's equations the gauged $\vec{T},\Phi - \Phi$ potential formulation can be derived as well, but in this case the equation of the magnetic field intensity can be separated into two different parts [7-8] as

(21) $$\vec{H} = \vec{T}_0 + \vec{H}_{\mathrm{m}},$$

where $\vec{T}_0$ current vector potential can be described by

(22) $$\nabla \times \vec{T} = \vec{J}_0,$$

and $\vec{H}_{\mathrm{m}}$ magnetic field intensity can be described by

(23) $$\nabla \times \vec{H}_m = \vec{0},$$

and

(24) $$\vec{H}_{\mathrm{m}} = -\nabla \Phi.$$

By applying (7) and (22) equations the electric field intensity can be obtained,

(25) $$\vec{E} = \frac{1}{\sigma} \nabla \times \vec{T}.$$

The following partial differential equations can be obtained employing (4), (6) and (24), where Coulomb gauge is satisfied

(26) $$\nabla \times \left(\frac{1}{\sigma} \nabla \times \vec{T}\right) - \nabla\left(\frac{1}{\sigma} \nabla \times \vec{T}\right) + \mu_0 \mathrm{j}\omega \vec{T} - \mu_0 \mathrm{j}\omega \Phi = -\mu_0 \mathrm{j}\omega \vec{T}_0 \text{ in } \Omega_{\mathrm{c}},$$

and

(27) $$\nabla \cdot \left(\mu_0 \vec{T} - \mu_0 \nabla \Phi\right) = -\nabla \cdot \left(\mu_0 \vec{T}_0\right) \text{ in } \Omega_{\mathrm{c}}.$$

The weak formulations from (26) and (27) partial differential equations in the case of the gauged $\vec{T},\Phi-\Phi$ potential formulation are the follows:

$$\int_{\Omega_c}\left[\frac{1}{\sigma}\left(\nabla\times\vec{W}\right)\cdot\left(\nabla\times\vec{T}\right)\frac{1}{\sigma}\left(\nabla\cdot\vec{W}\right)\cdot\left(\nabla\cdot\vec{T}\right)\right]\mathrm{d}\Omega$$

$$(28)+\int_{\Omega_c}\mu_0\vec{W}\mathrm{j}\omega\vec{T}-\mu_0\vec{W}\mathrm{j}\omega\nabla\Phi\ \mathrm{d}\Omega$$

$$=\int_{\Omega_c}\mu_0\vec{W}\mathrm{j}\omega\vec{T}_0\mathrm{d}\Omega$$

and

$$\int_{\Omega_c}\mu_0\mathrm{j}\omega\vec{T}\cdot\nabla\vec{N}\,\mathrm{d}\Omega-\int_{\Omega_c}\mu_0\nabla\vec{N}\cdot\nabla\mathrm{j}\omega\Phi\ \mathrm{d}\Omega$$

$$(29)\quad -\int_{\Omega_n}\mu\nabla\vec{N}\cdot\nabla\mathrm{j}\omega\Phi\ \mathrm{d}\Omega$$

$$=\int_{\Omega_c}\mu_0\mathrm{j}\omega\vec{T}_0\cdot\nabla\vec{N}\,\mathrm{d}\Omega-\int_{\Omega_n}\mu\mathrm{j}\omega\vec{T}_0\cdot\nabla\vec{N}\,\mathrm{d}\Omega.$$

The reduced magnetic scalar potential Φ can be described in the nonconducting domain Ω_n and in the conducting domain Ω_c as well, and the $\vec{T}$ current vector potential can be described only the Ω_c conducting domain.

From the Maxwell's equations the ungauged $\vec{T},\Phi-\Phi$ potential formulation can be derived the similar way. In this case the (27) equation is not changed. In the case of the ungauged $\vec{T},\Phi-\Phi$ potential formulation the Coulomb-gauge is satisfied automatically, consequently (26) is changed as [7-8]

$$(30)\quad \nabla\times\left(\frac{1}{\sigma}\nabla\times\vec{T}\right)+\mu_0\mathrm{j}\omega\vec{T}-\mu_0\mathrm{j}\omega\Phi$$

$$=-\mu_0\mathrm{j}\omega\vec{T}_0\ \text{in}\ \Omega_c.$$

The weak formulations the (26) and (27) partial differential equations in the case of the ungauged $\vec{A},V$ - $\vec{A}$ potential formulation are the follows:

$$\int_{\Omega_c}\left[\frac{1}{\sigma}\left(\nabla\times\vec{W}\right)\cdot\left(\nabla\times\vec{T}\right)\right]\mathrm{d}\Omega$$

$$(31)\quad +\int_{\Omega_c}\mu_0\vec{W}\mathrm{j}\omega\vec{T}-\mu_0\vec{W}\mathrm{j}\omega\nabla\Phi\ \mathrm{d}\Omega$$

$$=\int_{\Omega_c}\mu_0\vec{W}\mathrm{j}\omega\vec{T}_0\ \mathrm{d}\Omega$$

The other weak form is equal to the equation (29).

Simulation results

The simulations were have been prepared with in the frame of the COMSOL Multiphysics software on a SUN server, which includes 2x2,6 GHz processor and 32GB memory. Design of the model is very simple by this software. For employing of the $\vec{T},\Phi-\Phi$ potential formulation, the nonconducting hole must be replaced with a conducting material, which has a very small conductivity. Only in this case can be the model calculated [9-11].

Fig. 3. shows the scheme of the model with the simulation places. The frequencies of the exciting coil are 50 and 200 Hz. The experimental data of the eddy current density and the magnetic flux density have been presented at specified locations. The eddy current density was simulated along the lines A3-B3, on the upper surface of the conductor and A4-B4 on the bottom surface of the conductor. The magnetic flux density was simulated along the lines A1-B1 and A2-B2 at the middle of the exciting coil and the conductor.

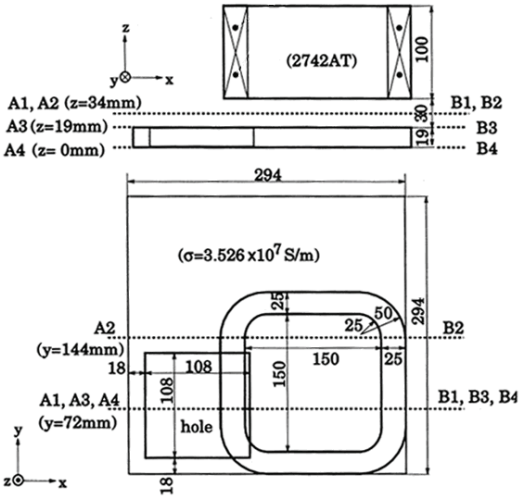

Fig.3. Computation model of Problem 7.

The simulation results were compared according to more viewpoints. The first one was comparing to the potential formulations with each others, considering their CPU times. The second was comparing to the potential formulations with each others, considering accuracy, with the measurement result. Table I shows the data of the simulation summed up, when the frequency is 50Hz.

Table 1. Parameters of the simulation (50Hz)

Method	$\vec{A},V$ - $\vec{A}$	$\vec{A},V$ - $\vec{A}$	$\vec{T},\Phi-\Phi$	$\vec{T},\Phi-\Phi$
	nodal	vector	nodal	vector
Frequency(Hz)	50	50	50	50
Degrees of freedom	684349	924130	274513	286186
Iteration	1524	195	386	328
CPU time (sec)	8223	1883	403	489

The CPU time was smaller when the $\vec{T},\Phi-\Phi$ potential formulations were employed, than in the case of the $\vec{A},V$ - $\vec{A}$ potential formulations, in 50Hz. Usage of the $\vec{T},\Phi-\Phi$ potential formulations were calculated with fewer degrees of freedom, like the $\vec{A},V$ - $\vec{A}$ potential formulations. The reason of the fewer degrees of freedom is that in the case of employing the $\vec{T},\Phi-\Phi$ potential formulations, in the non-conducting domain can be calculated with scalar variables. The Table II shows the data of the simulation summed up when the frequency is 200Hz.

Table 2.Parameters of the simulation (200Hz)

Method	$\vec{A},V$ - $\vec{A}$	$\vec{A},V$ - $\vec{A}$	$\vec{T},\Phi-\Phi$	$\vec{T},\Phi-\Phi$
	nodal	vector	nodal	vector
Frequency(Hz)	200	200	200	200
Degrees of freedom	684349	924130	274513	286186
Iteration	5403	204	420	400
CPU time (sec)	16102	1900	442	567

Using 200Hz the comparisons of the results were given similar results. The results were indicated, that with using $\vec{T}, \Phi - \Phi$ potential formulations in the simulation, are worthier because it gave the results faster. The density of the generated meshes was similar in cases of every simulation.

The other viewpoint was the correspondence with the results of the measurements. Fig. 4. shows the *z* component of the magnetic flux density, in the case of $\vec{A}, V$ - $\vec{A}$ potential formulations with 50Hz and 200Hz excitation compared with the measurement results as well.

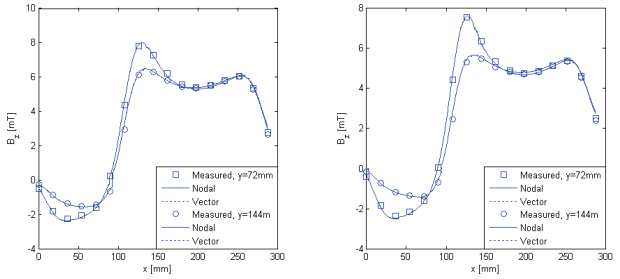

Fig.4. The comparison of the measurement results with the $\vec{A}, V$ - $\vec{A}$ simulation results

It is visible, that there isn't noticeable difference between accuracy of the several potential formulations.

Fig. 5. shows the *z* component of the magnetic flux density, in the case of $\vec{T}, \Phi - \Phi$ potential formulations with 50Hz and 200Hz excitation compared with the measurement results as well.

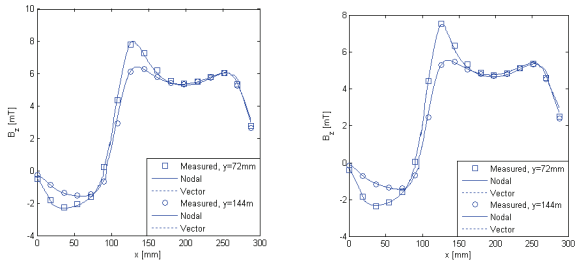

Fig.5. The comparison of the measurement results with the $\vec{T}, \Phi - \Phi$ simulation results

There is no noticeable difference between accuracy of the several potential formulations neither than the previously case.

Fig. 6. shows the *y* component of the changing of the eddy current in case of $\vec{A}, V$ - $\vec{A}$ potential formulations with 50 and 200 Hz excitation compared with the measurement results as well.

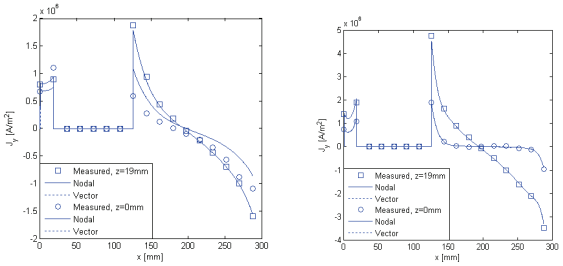

Fig.6. The comparison of the measurement results with the $\vec{A}, V$ - $\vec{A}$ simulation results

It is visible, that there is not noticeable difference between accuracy of the several potential formulations, like the previously case.

Fig. 7. shows the *y* component of the changing of the eddy current in case of $\vec{A}, V$ - $\vec{A}$ potential formulations with 50 and 200 Hz excitation compared with the measurement results as well.

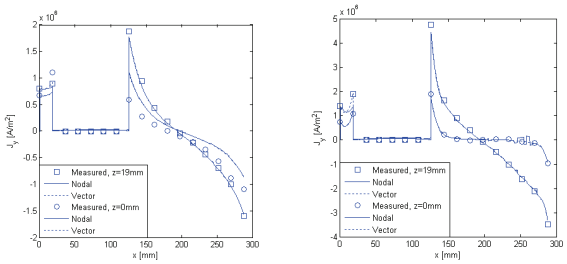

Fig.7. The comparison of the measurement results with the $\vec{T}, \Phi - \Phi$ simulation results

There is no noticeable difference between accuracy of the several potential formulations neither than the previously case.

The conclusion is that the simulation results are very similar to the case of using each potential formulation with the measurement results.

Simulation results

Some potential formulations were compared with each others, in connection with an international problem. With the usage of $\vec{T}, \Phi - \Phi$ formulations the results can be calculated faster, and the accuracy of the calculations was the same. So it seems that using $\vec{T}, \Phi - \Phi$ formulations are better, than the $\vec{A}, V$ - $\vec{A}$ formulation, but it is not easier, because when the $\vec{A}, V$ - $\vec{A}$ potential formulation should be used, the non-conducting hole must be replaced with a conducting material with very small conductivity. Only in this case can be the model calculated

REFERENCES

[1] www.compumag.org/jsite

[2] TEAM Workshops, Test Problems, 1988.

[3]http://www.cst.com/Content/Applications/Article/TEAM+Benchmark+7++Asymmetrical+conductor+model+with+a+hole

[4] Hajime Tsuboi, Motoo Tanaka, Kazumasa Ikeda, Kentaro Nishimura, Computation results of the TEAM workshop Problem 7 by Finite element methods using tetrahedral and hexahedral elements, *Journal of Materials Processing Technology*, vol. 108, 237--240, 2001.

[5] Fujiwara K., Nakata T., Results for benchmark problem 7. COMPEL, Vol. 11., pp. 335-344., 1990.

[6]M. Kuczmann, Nodal and Edge Finite Element Analysis of Eddy Current Field Problems, *Przegląd Elektrotechniczny*, vol. 84, no. 12, 2008, pp. 194-197.

[7] Kuczmann M., Iványi A., The finite element method in magnetics, *Academic Press*, Budapest, 2009.

[8] O. Bíró, Edge Element Formulations of Eddy Current Problems, *Comput. Meth. Appl., Mech. Engrg.*, vol. 169, 391--405, 1999.

[9] Comsol Multiphysics, www.comsol.com.

[10] I. F. Hantila, Mathematical Model of the Relation Between B and H for Non-linear Media, Revue Roumaine Des Sciences Techniques, *Electrotechnique et Energetique*, Bucarest, vol. 19, pp. 429--448, 1974.

[11] O. Bíró, K. Preis, and K. R. Richter. On the use of the magnetic vector potential in the nodal and edge finite element analysis of 3d magnetostatic problems. *IEEE Trans. on Magn.*, pages 651-654, 1996.

***Authors**: Gergely Kovács, E-mail: kovacs.gergely1984@gmail.com, dr. Miklós Kuczmann, E-mail: kuczmann@sze.hu; Department of Telecommunications, Laboratory of Electromagnetic Field, Egyetem tér 1, H-9026, Győr, Hungary.*